

A New Correction Factor-based Strategy with DWT-SVD for Contrast Enhancement in Digital Mammograms

Dharmendra Kumar^{*1,3}, Anil Kumar Solanki², Anil Kumar Ahlawat³

Submitted: 22/12/2023 Revised: 28/01/2024 Accepted: 08/02/2024

Abstract: Globally, breast cancer stands as the second most prevalent disease affecting women. Mammography, utilizing low-dose X-rays, remains a highly effective modality for the early detection of cancer. Challenges such as uneven illumination and machine-imposed limitations contribute to low-contrast mammogram images, potentially impacting the accuracy of diagnoses. Due to the inherently narrow intensity range in mammography images, distinguishing between cancerous and non-cancerous tissues becomes challenging. This paper introduces a novel approach that combines Adaptive Gamma Correction with a two-way Discrete Wavelet Transform-Singular Value Decomposition (DWT-SVD) to enhance the visual clarity of the resulting images while preserving crucial clinical information. The introduction of a new correction adjustment factor enhances the singular value of the image, resulting in a significantly improved contrast-enhanced output. Experimental validation is conducted using mini-MIAS dataset, assessing the proposed technique with quantitative parameters such as Structural Similarity Index Measurement (SSIM), Pearson Correlation Coefficient (PCC), Peak to Signal Noise Ratio (PSNR), Contrast Improvement Index (CII), Mean Absolute Error (MAE), and Average Mean Brightness Error (AMBE). The obtained average values, including scores of 0.929, 0.998, 22.875, 1.136, 14.457, and 14.138, respectively, demonstrate promising results compared to conventional methods. Furthermore, comparison with the state-of-the-art techniques shows improved results, showcasing significant advancements in local information preservation and contrast enhancement in mammography images.

Keywords: Mammograms, Contrast Enhancement, Discrete Wavelet Transform, Adaptive Gamma Correction, Singular Value Decomposition

1. Introduction

The need to address breast cancer, the leading cause of death for women, has spurred a creative explosion in research and diagnostic techniques in the rapidly changing field of medicine. In recent decades, there has been a dramatic increase in the consensus on the critical role that early intervention plays in improving patient survival rates[1], [2]. A wide range of imaging modalities, including magnetic resonance imaging (MRI), positron emission tomography (PET), ultrasonography, histology, computed tomography (CT), and X-rays, are woven into the complex fabric of breast cancer detection. Mammography is at the forefront of these modalities and is characterized by its unmatched cost-effectiveness and reliability[3]. However, low brightness and poor contrast, which hinder early disease identification, continue to pose a major hurdle to the visibility of tumors in mammography. Uneven illumination from imaging devices and inadequate lighting conditions exacerbate the loss of brightness in mammogram images, making it more difficult to discern minute features that are essential for

precise visual perception during mammography examinations[4], [5]. Acknowledging this crucial constraint, mammography improvement becomes a crucial aspect of medical imaging. This entails both noise reduction and a sophisticated contrast enhancement strategy, with the goal of revealing critical characteristics that are critical for the successful identification of anomalies in mammograms.

Histogram Equalization (HE) is commonly utilized for its simplicity and effectiveness in contrast enhancement, remapping gray levels based on input probability distributions. However, its limited usage stems from the tendency to flatten histograms, resulting in significant brightness changes and unwanted artifacts[6], [7]. To solve this problem, Contrast-Limited Adaptive Histogram Equalization (CLAHE) divides the image into many tiles and applies the same transformation algorithm used in HE to each tile independently. Furthermore, CLAHE redistributes the resulting histogram within the clip limit. Despite its advantages, CLAHE can over-enhance images, especially in areas with sudden grayscale changes, resulting in false borders and unwanted distortions[8].

To solve the above issues, BBHE presents a distinctive strategy, segmenting an input image's histogram into two sub-histograms based on its mean and independently equalizing them, thereby effectively preserving the original brightness[9]. Wan et al.[10] extended this

¹Research Scholar, Dr. APJ Abdul Kalam Technical University, Lucknow, India

²Bundelkhand Institute of Engineering and Technology, Jhansi, India

³KIET Group of Institutions, Ghaziabad, India

1 malik.dharam@gmail.com

2. solankibiet13@gmail.com

3. anil.ahlawat@kiet.edu

concept with Dualistic Sub-Image Histogram Equalization (DSIHE), utilizing median-based segmentation. While DSIHE suits non-uniform intensity distribution images, its brightness preservation potential is relatively modest. However, both BBHE and DSIHE techniques exhibit limitations in scenarios with complex image content or extreme brightness variations. Chen et al. [11] extended the BBHE approach by developing RMSHE, which generalizes the notion by recursively dividing each sub-histogram into two depending on mean intensity. This process continues until optimal enhancement is achieved. However, a notable drawback of this approach is its time complexity, attributed to the recursive process. Fuzzy systems have been introduced to automate clip limit selection based on image characteristics, enhancing contrast without compromising image quality [12]. Histogram Modified CLAHE (HM-CLAHE), a novel technique for adjusting contrast enhancement levels, was recently developed by Sundaram et al.[13]. Performance is assessed using metrics like Enhancement Measure (EME). This modification was required since CLAHE by itself had difficulty maintaining local information in mammograms. Subsequently, in their work, Sundaram et al. [14] used HM-LCE for mammography images in their study, which considerably improved local details by modifying the histogram of the original image using a modification function. Even with these improvements, the technique is still unable to fully capture all of the image's subtle elements. Nonlinear unsharp masking (NLUM) offers an approach that requires no prior knowledge of the image content [15].

Huang et al.[16] introduced the Adaptive Gamma Correction and Weighting Distribution (AGCWD) technique, employing an adaptive gamma correction and weighting distribution function to automatically enhance the brightness of dimmed images. While AGCWD offers a straightforward and effective contrast enhancement, its performance may be compromised when the input image lacks a sufficient number of bright pixels. Several studies have proposed hybrid histogram-based approaches combining gamma correction with traditional histogram equalization to maintain histogram statistics while altering the transformation curve[17], [18].To address the above mentioned problem, a fuzzy systems have been introduced to automate clip limit selection based on image characteristics, enhancing contrast without compromising image quality. The method (FC-CLAHE) is capable of achieving significant contrast enhancement while preserving brightness[19]. The paper presents a new method called Fuzzy Weighted Histogram Equalisation (FWHE) to improve the contrast of mammography images, which is essential for the early identification of breast cancer. FWHE produces best outcomes by undergoing three stages: fuzzy transformation, PDF

modification, and de-fuzzification. This process effectively enhances contrast, resulting in increased visual quality [20].

Since none of the aforementioned techniques can increase contrast locally, crucial concealed information may occasionally remain hidden. In the context of local contrast, a method for improving medical images using gradient modulation and luminance-level modulation was developed by Zhao et al.[21]. Demirel et al.[22] pioneered the utilization of the DWT-SVD technique for satellite image enhancement. The method entails utilizing SVD on the input image and subsequently improving the outcome using GHE. More precisely, SVD is utilized on the low-frequency LL sub-band acquired by DWT. This process produces a new LL sub-band by multiplying correction coefficients with the matrix of singular values. The ultimate equalized satellite image is achieved by applying inverse DWT, resulting in a considerably enhanced image with increased contrast and clarity. On the other hand, Kallel et al. [23] created a technique especially designed for low-contrast CT images that uses DWT-SVD and adaptive gamma correction. It should be noted that this method might not work as well for some other kinds of medical images[17], [24]. Luminance control techniques focusing on value channels in color spaces have been proposed, utilizing gamma correction and contrast enhancement methods like CLAHE to improve image quality [25]–[27]. Generalized contrast enhancement using gray level S-Curve transformation has been explored, though it sometimes introduces blocking artifacts [28]. A multi-objective genetic algorithm has been used to modify local S-Curve transformations [29].

Numerous contrast enhancement techniques [30]–[33] have been developed to address issues such as contrast improvement, brightness preservation, edge retention, and artifact reduction. However, some techniques solely enhance image contrast without improving information content. Others may achieve better contrast but fall short in preserving brightness and structure similarity. Certain methods lack adaptability and result in artifacts. The effectiveness of an enhancement technique lies in its adaptability and the ability to strike a proper balance among these parameters, ensuring improved information content, brightness preservation, edge retention, and artifact reduction in enhanced medical images. Hence, the pursuit of an adaptive and effective enhancement technique tailored for medical images is crucial.

The literature review indicates that maintaining the naturalness of the original mammography while enhancing contrast without artifacts or losing relevant information is still a challenge. To deal with the above stated problem we introduce a novel approach that combines Adaptive Gamma Correction with a two-way

DWT-SVD to enhance the visual clarity of the resulting images while preserving crucial clinical information. The Discrete Wavelet Transform (DWT) is a common method for converting images from the spatial domain to the frequency domain, yielding four frequency sub-bands: LL, LH, HL, and HH [34]. In our distinct approach, we prioritize the preservation of edge details by exclusively concentrating on the LL sub-band for contrast enhancement. Furthermore, the Singular Value Decomposition (SVD) technique is applied to generate a singular value matrix, involving the factorization of a matrix into three constituent matrices [35]. Notably, SVD is strategically employed on the LL sub-band to capture and utilize intensity information for effective image equalization. The introduction of a new correction adjustment factor enhances the singular value of the image, resulting in a significantly improved contrast-enhanced output. This harmonious integration of DWT and SVD ensures a sophisticated enhancement strategy, emphasizing the protection of crucial edge details while optimizing the overall contrast adjustment.

The major contribution of this research is:

- To introduce a novel approach for contrast enhancement in mammogram through the integration of adaptive gamma correction and DWT-SVD.
- The introduction of a new correction adjustment factor enhances the singular value of the image, resulting in a significantly improved contrast-enhanced output.
- To evaluate the proposed method on qualitative and on various quantitative measures comparing it with both conventional and state-of-the-art methods, utilizing the mini MIAS dataset.

This paper is structured in the following manner: In Section 2, the proposed enhancement model is explained, and the experimental results and discussion are shown in Sections 3. Finally, Section 4 presents the research conclusion.

2. Proposed Research Methodology

Mammogram Images suffered from low brightness and poor contrast, which hinder early disease identification, continue to pose a major hurdle to the visibility of tumors in mammography. Therefore, we use an approach that combines Adaptive Gamma Correction with a two-way DWT-SVD to enhance brightness and contrast, resulting images with visual clarity while preserving crucial clinical information.

2.1 Contrast-Limited Adaptive Histogram Equalization (CLAHE)

CLAHE is a powerful image processing technique designed to enhance local contrast, particularly effective in medical imaging. Contrary to conventional Histogram Equalization (HE), CLAHE can adjust itself according to the distinct attributes of different areas in an image. This adaptability is crucial for maintaining details in areas with diverse intensity levels. The method involves dividing the image into small regions called tiles and applying standard histogram equalization independently to each tile. The limiting factor, termed the "clip limit," prevents over-amplification of intensities during the equalization process, ensuring the preservation of image details. Mathematically, CLAHE can be expressed as:

$$f(x_i) = x_0 + (x_{L-1} - x_0) \cdot C(x_i), \quad i = 0, 1, 2, \dots, L-1 \quad (1)$$

In this equation $f(x_i)$ embodies the transformed pixel intensity, $C(x_i)$ presents the cumulative density function corresponding to x_i , x_i signifies the specific input image intensity, and L signifies the total number of intensity levels. This adaptive strategy underscores CLAHE's efficacy in averting over-enhancement risks while significantly augmenting contrast, rendering it particularly well-suited for diverse applications in image analysis, especially within the intricate domain of medical imaging.

2.2 Adaptive Gamma Correction

Mammogram images often face challenges with inadequate brightness, attributed to uneven illumination from imaging instruments and inadequate lighting settings. This limitation hinders the detection of subtle details during mammogram screenings, impacting visual perception. Consequently, there is a crucial demand to improve luminosity, aiming to enhance the visual perception of mammogram images for more effective and accurate diagnosis. The utilization of adaptive gamma correction stands out as an effective computational technique for improving the visual information in images [26]. In a customized application, AGC has undergone modification specifically for mammography images. This adaptation involves the dynamic calculation of the intensity transformation function, aligning with the statistical characteristics inherent in mammographic data. The approach aims to optimize the enhancement process, recognizing the unique features and requirements of mammogram images for improved visual representation.

This approach presents a systematic procedure for implementing adaptive gamma correction, taking into account the weighting factor determined by the probability density function. Pixel values in the image are adjusted individually to improve the contrast of mammograms adaptively. The method of adaptive gamma correction is outlined in the following steps:

Step 1: Calculate the histogram of the mammogram, separating the probability of each pixel value to be within each bin in the range [0-255].

Step 2: Identify the highest and lowest values among the probability counts in the image.

Step 3: For each pixel value x in the range [0-255], calculate the weighting factor $W(x)$ using the equation:

$$W(x) = \frac{\sum_{j=0}^x pdf_w(j)}{\sum_{j=0}^{mVal} pdf_w(j)} \quad (2)$$

Where $pdf_w(j)$ represents the probability function of pixel value j .

Step 4: Apply adaptive gamma correction for each pixel value j (0 to 255) in the image:

$$x(j) = x_{max} \cdot \left(\frac{x(j)}{mVal}\right)^{1-w(j)} \quad (3)$$

Where x_{max} is the maximum pixel value.

2.3 Contrast enhancement by DWT-SVD

DWT serves as a highly effective computational tool in image processing, breaking down the input image into four decomposed sub-band images: LL, LH, HL, and HH frequency groups [34]. This approach excels in obtaining localized information for high-level signal or image processing tasks. The LL sub-band captures low-frequency details, while the other sub-bands focus on edges. By dividing high-frequency sub-bands and applying illumination enhancement and thresholding with optimized values specifically in the LL sub-bands, the method ensures the preservation of edge details while minimizing distortion. Subsequently, the enhanced image is obtained through the application of inverse DWT. Furthermore, the Singular Value Decomposition (SVD) technique is applied to generate a singular value matrix, involving the factorization of a matrix into three constituent matrices[35]. Notably, SVD is strategically employed on the LL sub-band to capture and utilize intensity information for effective image equalization. The comprehensive explanation of the suggested technique is depicted in Fig 1.

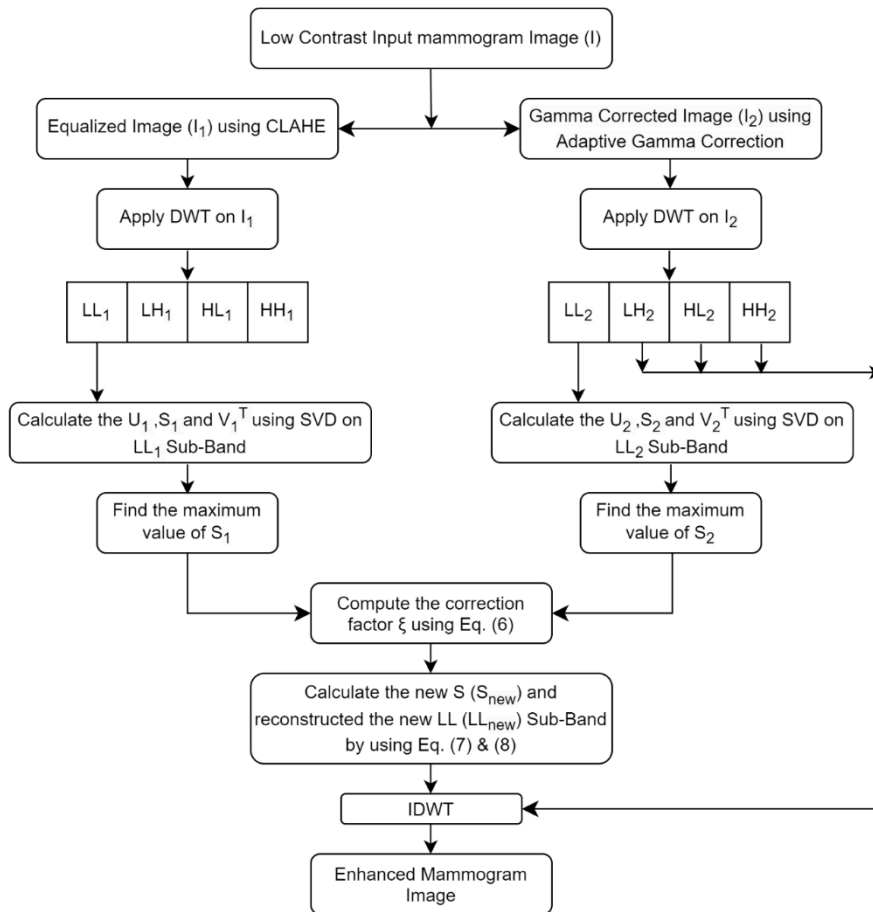


Fig 1 Detailed steps of the proposed technique

The low-contrast mammography image enhancement algorithm consists of multiple sequential phases. The equalized image (I_1) is first obtained by applying CLAHE on the input image (I). Concurrently, the original image (I) undergoes an adaptive gamma correction to produce the gamma-corrected image (I_2). The low-frequency sub-band LL_1 and LL_2 are then produced by separately applying a one-level DWT to I_1 and I_2 . Equations (4) and (5) provide the matrices respectively, when the SVD operation is carried out independently on these low-frequency sub-bands.

$$LL_1 = U_1 \cdot S_1 \cdot V_1^T \quad (4)$$

$$LL_2 = U_2 \cdot S_2 \cdot V_2^T \quad (5)$$

Next, using Equation (6), calculate the correction adjustment factor

$$\xi = \frac{\max(S_1) + \max(S_2)}{2 \cdot \max(S_2)} \quad (6)$$

Equation (7) provides a modified singular matrix S_{new} , which is generated using this factor.

$$S_{new} = \xi \cdot S_2 \quad (7)$$

$$LL_{new} = U_2 \cdot S_{new} \cdot V_2^T \quad (8)$$

The inverse SVD procedure is used to produce the improved sub-band of the low-frequency component (LL_{new}) by using Equation (8). The changed sub-band LL_{new} and the sub-bands LH_2 , HL_2 , and HH_2 are then subjected to an inverse DWT, which produces the enhanced image.

3. Performance Evaluation and Results

The empirical results of our proposed approach are shown in this section along with a comparison analysis of it against other conventional techniques including BBHE, HE, AGCWD, CLAHE, and DSHIE. To assess the efficacy of our approach, we expand the evaluation to include cutting-edge techniques, all of which have been re-implemented using the same framework and dataset. The solution we present effectively resolves image enhancing issues while successfully attaining the target level of improvement. The algorithm's performance is thoroughly assessed using a comprehensive

mammography dataset (1024x1024) obtained from mini-MIAS [36]. The dataset consists of 322 images. To be concise, the results primarily concentrate on six sample images that represent different categories such as fatty, fatty glandular, dense glandular, and so on. The proposed technique's hardware and software configuration is established on an Intel (R) Core (TM) i-3-1115G-4 CPU @ 3.00 GHz and MATLAB (R2019) implemented. Performance is demonstrated by evaluating both the visual aesthetics and quantitative measurements of improved mammography pictures, rating their quality and effectiveness in reducing errors.

3.1 Qualitative Evaluation

The main objective of improving mammography is to detect malignant tissue inside the image. Uneven illumination and limitations in image capture are contributing factors to the production of low-contrast pictures, potentially impacting the accuracy of mammogram diagnoses. Consequently, effective contrast enhancement becomes crucial to visually present the resulting image and preserve the clinical information. The proposed method undergoes evaluation through both visual and quantitative assessments, employing measures of image enhancement quality and error. In Fig. 3, low-contrast original mammogram images and their histograms are depicted, while Fig. 4(i)-(vi) showcases the enhanced mammogram images corresponding to Img-1, employing AGCWD, CLAHE, DSHIE, BBHE, HE, and the proposed methods, along with their respective histograms. Fig. 4 highlights that the proposed technique yields perceptually superior results, preserving critical information in the enhanced image. Notably, AGCWD in Fig. 4(i) exhibits over-enhancement, potentially leading to misconceptions in the mammogram image. CLAHE and BBHE in Fig. 4(ii) and Fig. 4(iv) provide high contrast but introduce noise. DSHIE in Fig. 4(iii) lacks perceptual quality due to insufficient edge preservation. The resulting image from HE in Fig. 4(v) is overly bright, indicated by a high AMBE value. In contrast, the strategy presented in Figure 4(vi) demonstrates superior visual performance compared to conventional methods by improving local characteristics and retaining edge details. Fig. 4 displays histograms of the improved images employing different techniques, including the suggested approach.

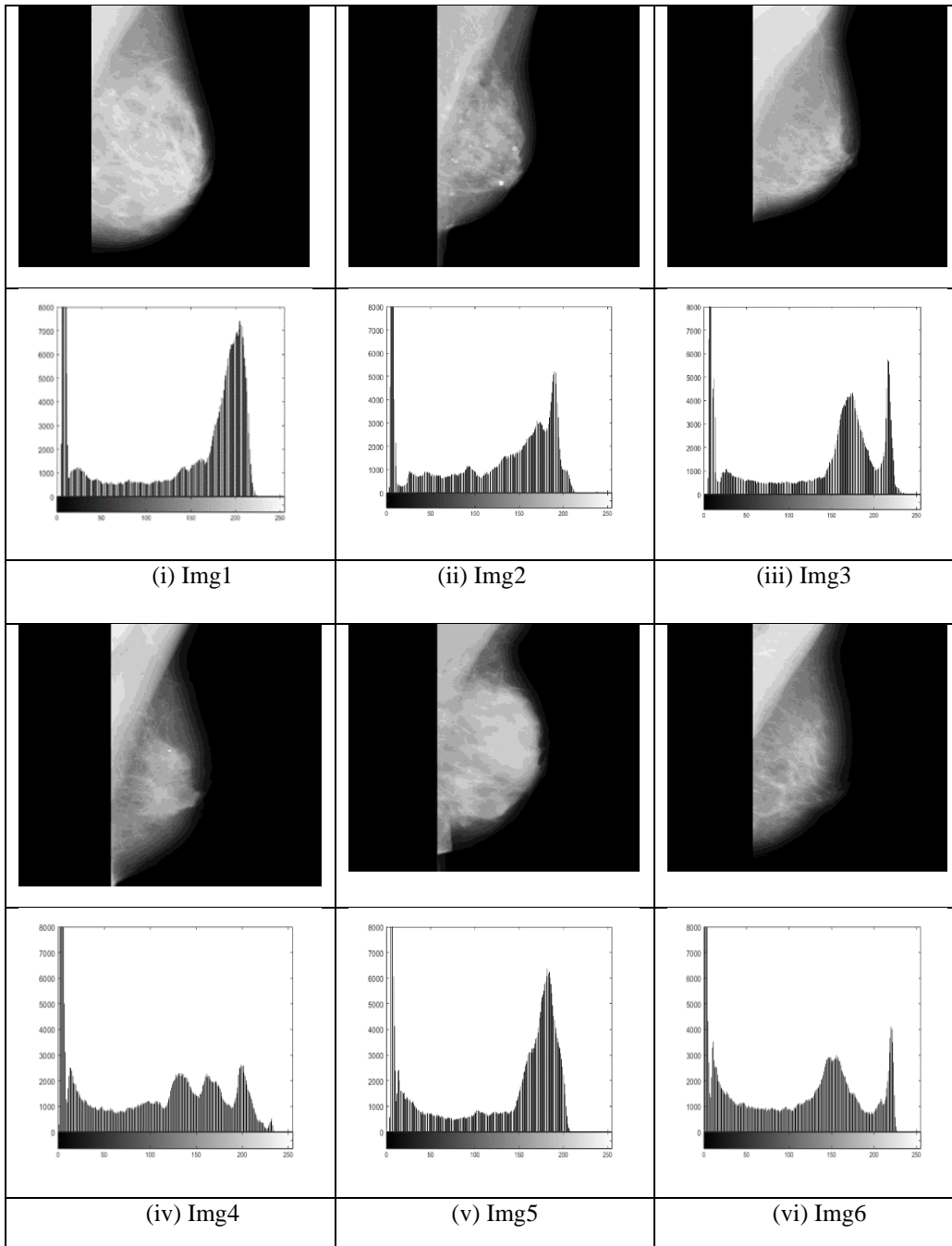
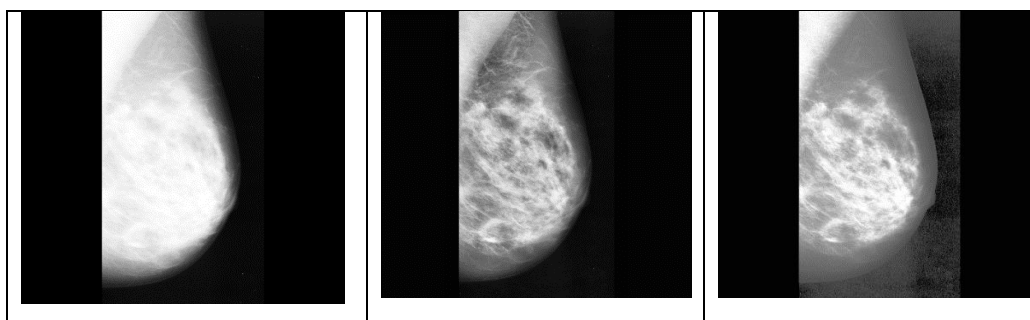


Fig 3 Original Mammogram Images (Img1 to Img6) and their corresponding histogram



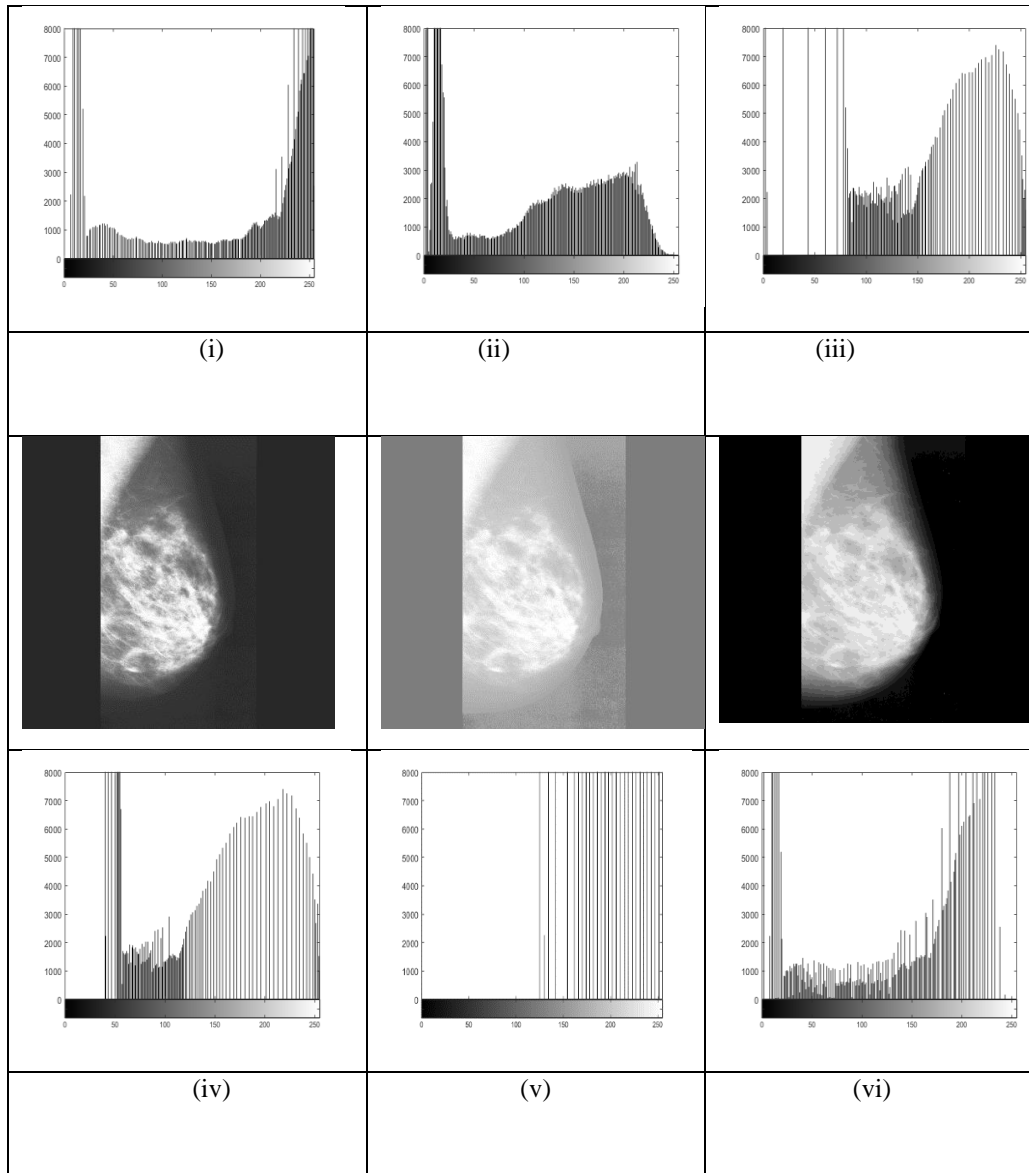


Fig 4 Contrast Enhanced mammogram image (Img1) with corresponding histogram (i) with AGCWD (ii) with CLAHE (iii) with DSIHE (iv) with BBHE (v) with HE (vi) with Proposed Technique

3.2 Quantitative Evaluation

In this section the effectiveness of the proposed technique using different quantitative metrics is illustrated. The quantitative analysis is divided into two distinct categories. The enhanced image's quality is assessed based on parameters such as SSIM, PCC, PSNR, and CII. Nevertheless, the process of error estimate is conducted by employing the MAE and AMBE. The summary of all the assessment criteria is provided below:

Quality Evaluation Metrics:

- **Structural Similarity Index Measurement (SSIM):** SSIM evaluates image quality by comparing the structural similarity between the original and enhanced images, focusing on luminance (L), contrast (C), and structure (S) components[37].

$$SSIM = \frac{(2\mu_x\mu_y+C_1)(2\sigma_x\sigma_y+C_2)(\sigma_{xy}+C_3)}{(\mu_x^2+\mu_y^2+C_1)(\sigma_x^2+\sigma_y^2+C_2)} \quad (9)$$

where μ_x, μ_y , are the local means, σ_x, σ_y are the standard deviations, and σ_{xy} cross-covariance for images x, y . Higher SSIM values correspond to superior performance in terms of image quality.

- **Pearson Correlation Coefficient (PCC):** PCC measures the correlation degree between the pixel intensities of the original and enhanced images, with a range from 0 (no correlation) to 1 (perfect correlation)[38].

$$PCC = \frac{\sum_{i=1}^m \sum_{j=1}^n ((x(i,j)-\bar{x})(y(i,j)-\bar{y}))}{\sqrt{\sum_{i=1}^m \sum_{j=1}^n (x(i,j)-\bar{x})^2} \sqrt{\sum_{i=1}^m \sum_{j=1}^n (y(i,j)-\bar{y})^2}} \quad (10)$$

Where \hat{x} and \hat{y} represent the average of sample x and sample y .

- *Peak signal-to-noise ratio (PSNR)*: PSNR quantifies the ratio of the maximum possible power of a signal to the power of corrupting noise that affects the fidelity of its representation[37].

$$PSNR = 10 \log_{10} \frac{(L - 1)^2}{MSE} \quad (11)$$

Thus, L is an image's maximum number of intensity levels that can exist.

$$MSE = \frac{1}{mn} \sum_{i=0}^{m-1} \sum_{j=0}^{n-1} (O(i, j) - D(i, j))^2 \quad (12)$$

Where, $O(i, j)$ refers to the original image's matrix data. $D(i, j)$ refers to the segmented image's matrix data

- *Contrast Improvement Index (CII)*: CII assesses contrast enhancement by comparing the average local contrast of the original and processed images, with higher scores indicating better image quality[23].

$$CII = \frac{C_o}{C_i} \quad (13)$$

C_i represents the mean intensity of local contrast in the input image, whereas C_o represents the mean intensity of local contrast in the output image.

Error Estimation Metrics:

- *Average Mean Brightness Error (AMBE)*: AMBE determines brightness preservation by quantifying the absolute error in brightness between the original and enhanced images, with lower values indicating less information loss[38].

$$AMBE = |E[Y] - E[X]|$$

$E[Y]$ and $E[X]$ represent the average gray levels of the enhanced and input image, respectively.

- *Mean Absolute Error (MAE)*: This parameter, while not explicitly defined in the quoted text, is typically used to measure the average pixel-wise discrepancy between the enhanced and original images, aiming for lower values for higher fidelity.

$$MAE = \frac{1}{mn} \sum_{i=1}^m \sum_{j=1}^n |Y(i, j) - X(i, j)|$$

Where X and Y denote the input and enhanced images, respectively, both having dimensions (m, n) .

The utilization of these matrices in the performance assessment of the proposed scheme ensures a robust and comprehensive evaluation, focusing on both the enhancement of image quality and the minimization of information loss.

Table 1 Comparative analysis based on SSIM, PCC, PSNR, CII, MAE, and AMBE metric

Image	SSIM	PCC	PSNR	CII	MAE	AMBE
Img1	0.9163	0.9987	21.9831	1.1788	15.5932	15.4972
Img2	0.9172	0.9979	21.8542	1.0925	14.1328	14.0323
Img3	0.9255	0.9975	23.4802	1.0890	12.8465	12.8955
Img4	0.9179	0.9940	21.8925	1.1859	14.4978	14.0178
Img5	0.9357	0.9984	21.7847	1.1684	15.6991	15.3191
Img6	0.9178	0.9955	23.8000	1.1887	14.6033	14.5034
Average	0.9217	0.9970	22.4658	1.1505	14.5621	14.3775

The recommended approach is compared with various traditional approaches such as HE, AGCWD, CLAHE, DSIHE, and BBHE in Tables 2, 3, 4, 5, 6, 7, and Figures 5, 6, 7, 8, 9, 10. By implementing them in MATLAB with the chosen image database, the suggested method is compared with the conventional approaches. The results of employing the SSIM parameter to evaluate various techniques are displayed in Table 2. Notably, in

comparison to other procedures, the proposed procedure produces much better outcomes. The proposed approach resulted in six images with significantly higher average SSIM values, showing a substantial similarity between the improved and original images. Figure 5 illustrates the exceptional effectiveness of the suggested method on the complete dataset of 322 mammography images.

Table 2 Comparative analysis based on SSIM metric

Image	HE	AGCWD	CLAHE	DSIHE	BBHE	Proposed Method
Img1	0.2130	0.9114	0.3115	0.2382	0.2282	0.9163
Img2	0.1442	0.9156	0.2398	0.8142	0.2345	0.9172
Img3	0.1580	0.9217	0.2424	0.8101	0.2110	0.9255
Img4	0.1099	0.9100	0.2304	0.8339	0.2425	0.9179
Img5	0.1688	0.9352	0.2399	0.8086	0.1927	0.9357
Img6	0.1236	0.9135	0.2334	0.8445	0.2365	0.9178
Average	0.1529	0.9179	0.2496	0.7249	0.2242	0.9217

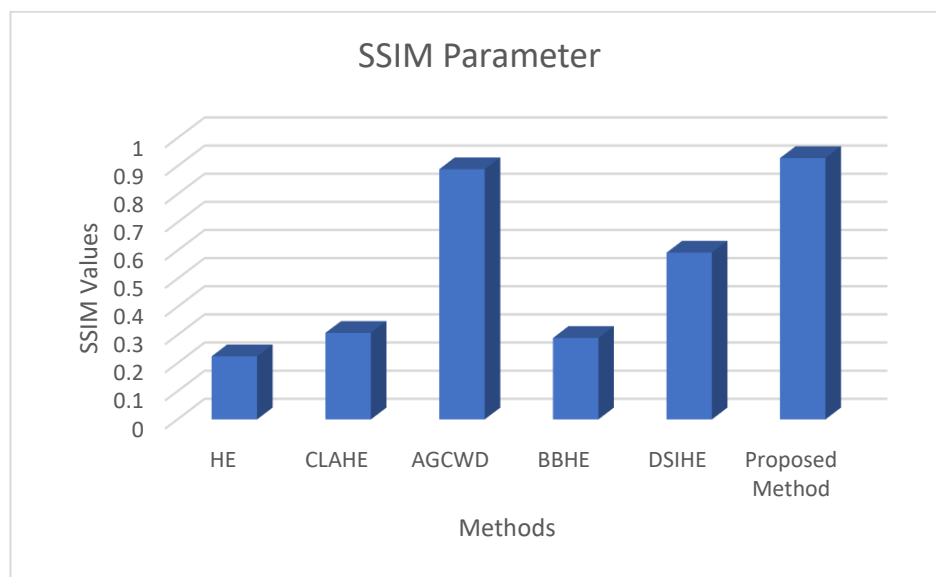


Fig 5 SSIM parameter based graphical comparison on mini MIAS Dataset (all 322 images)

Table 3 comparisons highlight key findings in various histogram equalization methods. BBHE shows the lowest average PCC (0.9644), followed closely by DSHIE (0.9712). HE and DSHIE exhibit similar PCC values (0.9745 and 0.9712). The proposed technique achieves an exceptionally high average PCC (0.9970), demonstrating a superior correlation with the original image. In general,

the improved images generated by the suggested technique consistently exhibit stronger correlation when compared to other methods, as indicated in Table 3. The proposed method exhibits remarkable linear consistency and correlation, as depicted in Figure 6, with notably higher average PCC values across 322 mammography images.

Table 3 Comparative analysis based on PCC metric

Image	HE	AGCWD	CLAHE	DSIHE	BBHE	Proposed Method
Img1	0.9650	0.9978	0.9857	0.9638	0.9453	0.9987
Img2	0.9746	0.9975	0.9853	0.9678	0.9697	0.9979
Img3	0.9764	0.9966	0.9906	0.9736	0.9573	0.9975
Img4	0.9705	0.9939	0.9742	0.9689	0.9838	0.9940
Img5	0.9767	0.9983	0.9822	0.9748	0.9474	0.9984
Img-6	0.9839	0.9923	0.9759	0.9784	0.9828	0.9955
Average	0.9745	0.9961	0.9823	0.9712	0.9644	0.9970

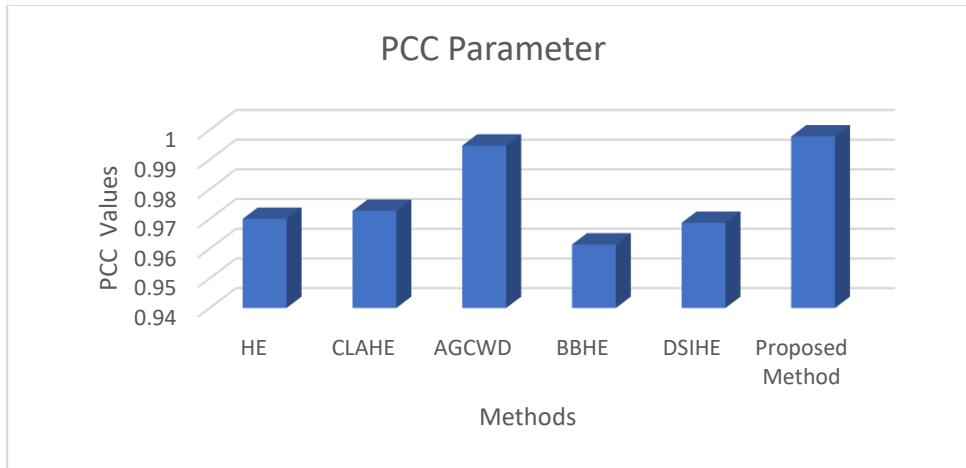


Fig 6 PCC parameter based graphical comparison on mini MIAS Dataset (all 322 images)

The proposed method consistently outperforms, demonstrating high PSNR values with an outstanding average of 22.4658. This surpasses traditional methods, with the closest competitor being CLAHE at an average PSNR of 23.1227. Figure 7 visually reinforces these

findings, illustrating the proposed method's marked improvement over HE and competitive performance compared to advanced methods like AGCWD, BBHE, and DSIHE.

Table 4 Comparative analysis based on PSNR metric

Image	HE	AGCWD	CLAHE	DSIHE	BBHE	Proposed Method
Img1	7.229734	16.53132	23.53779	19.56773	20.32687	21.98313
Img2	5.085276	19.17196	21.52823	19.04997	19.88251	21.85416
Img3	5.306343	17.77865	23.3725	20.24367	22.34395	23.48024
Img4	4.965226	20.05676	23.96056	19.17547	19.2457	21.89247
Img5	5.32347	17.6113	22.26418	18.72733	22.2	21.78468
Img6	4.923983	19.64347	24.07319	19.06998	20.93722	23.79997
Average	5.472339	18.46558	23.12274	19.30569	20.82271	22.46577

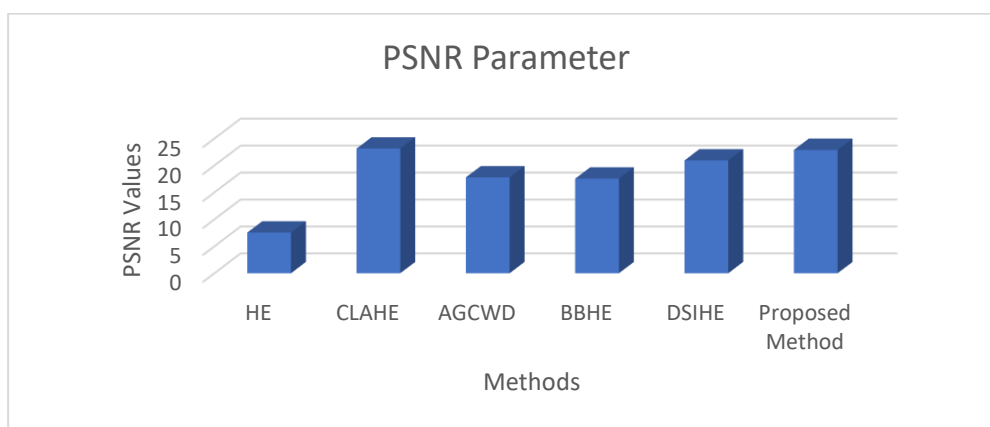


Fig 7 PSNR parameter based graphical comparison on mini MIAS Dataset (all 322 images)

The CII scores for DSIHE, AGCWD, and the suggested methodology exhibit relatively comparable values (Table 5). The average CII score for AGCWD (1.10979) is slightly inferior to that of our proposed

technique (1.1505). Our outcomes outshine those of HE, CLAHE, and BBHE, resulting in enhanced image quality compared to the original images. Analysis of the data illustrated in Figure 8 reveals that the mean CII score of

our suggested approach is marginally higher than that of alternative methods across all 322 images.

Table 5 Comparative analysis based on CII metric

Image	HE	AGCWD	CLAHE	DSIHE	BBHE	Proposed Method
Img1	0.5652	1.1087	1.0783	1.1000	0.9348	1.1788
Img2	0.4208	1.0625	1.0542	1.0625	0.9375	1.0925
Img3	0.5187	1.0581	1.0249	1.0581	0.9046	1.0890
Img4	0.4298	1.0851	1.0681	1.0851	0.9660	1.1859
Img5	0.4612	1.1644	1.0868	1.1644	1.0046	1.1684
Img6	0.4217	1.1087	1.0739	1.1087	0.9783	1.1887
Average	0.4696	1.0979	1.0643	1.0965	0.9543	1.1505

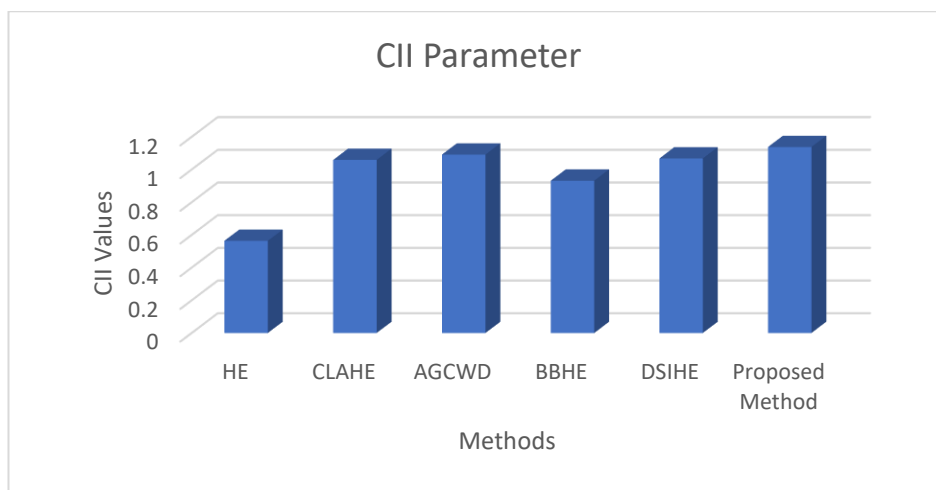


Fig 8 CII parameter based graphical comparison on mini MIAS Dataset(all 322 images)

The MAE parameter further highlights the superior performance of our proposed algorithm is documented in Table 6. Our method demonstrated an average MAE value of approximately 14.5621, outperforming BBHE, AGCWD, DSIHE, and HE methods with values of 29.3539, 14.8413, 14.6485, and 130.3735, respectively. The proposed method's average MAE (14.5621) closely

aligns with DSIHE (14.6485), yet it surpasses DSIHE, implying superior performance and minimal distortion in the enhanced images. Figure 10 graphically compares the MAE values on dataset (all 322 images). The proposed method's lowest MAE value shows its effectiveness in maintaining image fidelity during enhancement.

Table 6 Comparative analysis based on MAE metric

Image	HE	AGCWD	DSIHE	BBHE	Proposed Method
Img1	102.3144	16.0910	15.3703	36.4021	15.5932
Img2	137.2902	14.7741	14.3274	26.8607	14.1328
Img3	131.1784	13.1972	9.968609	31.3422	12.8465
Img4	139.9295	14.3150	16.5357	24.0376	14.4978
Img5	131.8405	15.9564	18.2331	32.3504	15.6991
Img6	139.6881	14.7140	13.4559	25.1304	14.6033
Average	130.3735	14.8413	14.6485	29.3539	14.5621

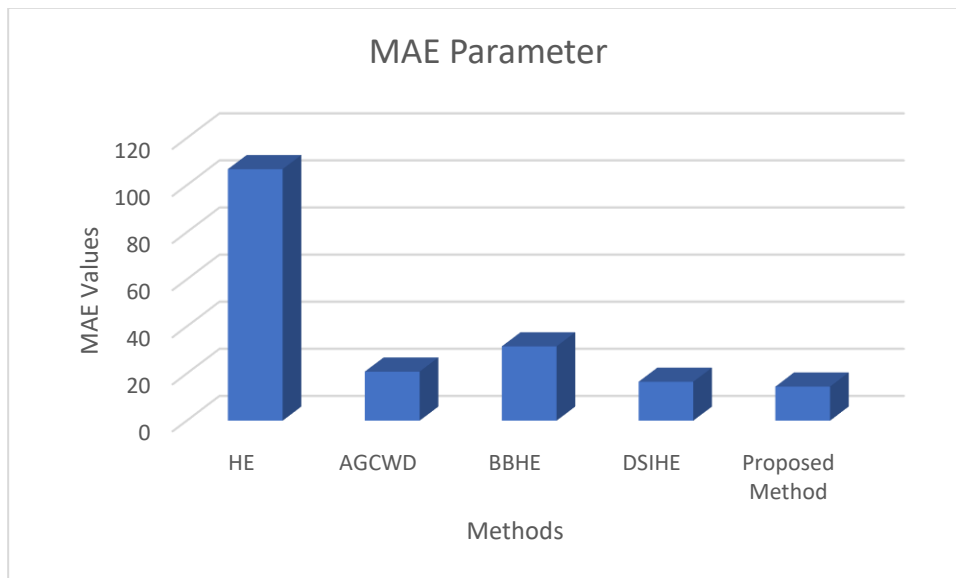


Fig 9 MAE parameter based graphical comparison on mini MIAS Dataset(all 322 images)

Table 7 demonstrates the higher performance of the suggested method, as evidenced by the lowest AMBE value (14.3775), which indicates improved preservation of brightness compared to the original image. The suggested strategy surpasses existing methods due to its continuously lower AMBE scores, which minimize information loss and result in superior enhancement. Fig 9 succinctly illustrates

the superior AMBE performance of the proposed method, showcasing its consistently lower values compared to other methods across all 322 mammogram images in the mini MIAS dataset. This graphical representation emphasizes the proposed method's effectiveness in preserving the original image's brightness and crucial diagnostic information.

Table 7 Comparative analysis based on AMBE metric

Image	HE	AGCWD	DSIHE	BBHE	Proposed Method
Img1	102.3144	16.0910	10.6427	21.4899	15.4972
Img2	137.2902	14.7741	14.3264	22.3837	14.0323
Img3	131.1784	13.1972	13.1731	21.5013	12.8955
Img4	139.9295	14.3150	16.5357	22.3325	14.0178
Img5	131.8405	15.9564	18.2297	23.1687	15.3191
Img6	139.6881	14.7140	13.4559	22.8224	14.5034
Average	130.3735	14.8413	14.3939	22.2831	14.3775

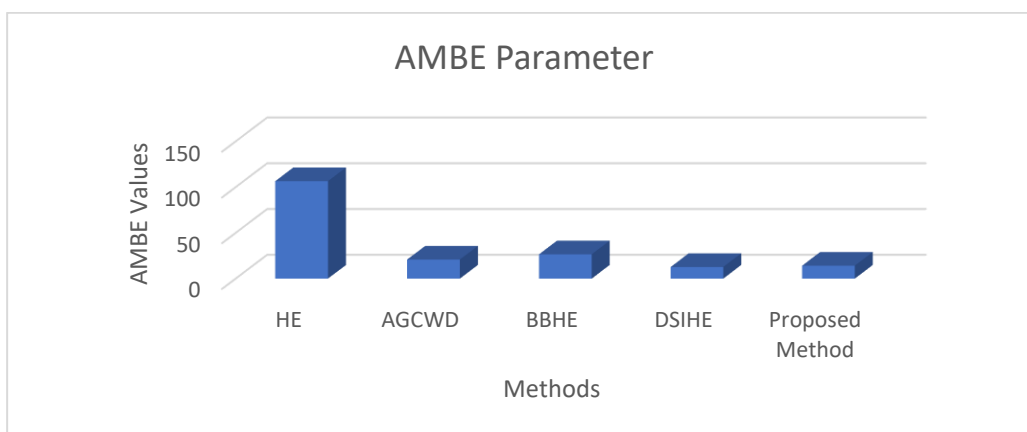


Fig 10 AMBE parameter based graphical comparison on mini MIAS Dataset(all 322 images)

Table 8. Quantitative Comparative analysis with state-of-art methods on mini MIAS dataset (all 322 Images)

Contrast Enhancement Technique	Performance Indicator					
	SSIM	PCC	PSNR	CII	MAE	AMBE
FC-CLAHE	0.716	0.934	17.138	2.983	28.303	12.207
FWHE	0.681	0.908	18.235	1.007	25.128	12.563
DWT-SVD	0.786	0.925	9.221	0.962	32.314	29.568
DWT-SVD-AGC	0.751	0.941	12.576	0.997	30.573	23.856
Proposed Method	0.929	0.998	22.875	1.1376	14.457	14.138

As delineated in Table 8, the proposed method notably achieved the highest average values for SSIM (0.929), PCC (0.998), PSNR (22.875), and CII (1.1376), which collectively indicate a robust enhancement of image quality while maintaining a high fidelity to the original image data. Concurrently, it maintained lower average values of AMBE (14.138) and MAE (14.457), signifying an optimal balance between contrast enhancement and naturalness preservation. In particular, the proposed method's PCC value exemplifies an exemplary correlation with the original imagery, towering over traditional methods, such as FWHE, which registered the lowest average PCC (0.908). Similarly, the SSIM and PSNR parameters, indicative of structural preservation and image clarity, respectively, were highest for the proposed method. Conversely, FWHE and DWT-SVD lagged behind with the lowest values for SSIM and PSNR, suggesting a less precise enhancement process. Notably, while FC-CLAHE achieved the highest CII average (2.983), the proposed method closely followed, ensuring a substantial improvement in image contrast without compromising detail. The AMBE and MAE parameters further establish the proposed method's proficiency, showcasing its capability to enhance contrast with minimal distortion — a critical factor in medical imaging where precision is paramount.

Conclusively, the proposed method outperforms established state-of-the-art methods across most parameters, with its least impressive values still falling within an optimal range. It holds a definitive edge in the enhancement of mammogram images, delivering high-quality, reliable results.

4. Conclusion

This study addresses the critical challenge of low-contrast mammogram images, which can impact the accuracy of breast cancer diagnoses. Through the introduction of a novel approach incorporating Adaptive Gamma Correction and a two-way DWT-SVD, our method

significantly enhances visual clarity while preserving crucial clinical information. The incorporation of a new correction adjustment factor is crucial in enhancing the singular value of the image, resulting in a significant improvement in contrast in the output. The experimental validation, performed on the mini-MIAS dataset, utilizes a range of quantitative measures including SSIM, PCC, PSNR, CII, MAE, and AMBE. The obtained results, outperform with conventional methods and demonstrate significant advancements compared to state-of-the-art techniques. This innovative approach, with its emphasis on local information preservation and contrast enhancement, holds considerable potential for aiding medical practitioners in the identification of cancerous locations during mammogram image screenings. Despite commendable performance, notable issues, such as the method's response to noise and lacking clinical evaluations, necessitate further exploration. Future endeavours involve assessing the method in diverse noisy environments through clinical trials, enhancing its applicability and robustness in real-world scenarios.

References

- [1] R. Mousa, Q. Munib, and A. Moussa, "Breast cancer diagnosis system based on wavelet analysis and fuzzy-neural," *Expert Syst. Appl.*, vol. 28, no. 4, pp. 713–723, 2005, doi: 10.1016/j.eswa.2004.12.028.
- [2] X. Gao, Y. Wang, X. Li, and D. Tao, "On combining morphological component analysis and concentric morphology model for mammographic mass detection," *IEEE Trans. Inf. Technol. Biomed.*, vol. 14, no. 2, pp. 266–273, 2010, doi: 10.1109/TITB.2009.2036167.
- [3] V. Bhateja, M. Misra, and S. Urooj, "Human visual system based unsharp masking for enhancement of mammographic images," *J. Comput. Sci.*, vol. 21, pp. 387–393, 2017, doi: 10.1016/j.jocs.2016.07.015.
- [4] T. Chaira, "Intuitionistic fuzzy approach for enhancement of low contrast mammogram images," *Int. J. Imaging Syst. Technol.*, vol. 30, no. 4, pp.

1162–1172, 2020, doi: 10.1002/ima.22437.

- [5] L. Sun *et al.*, “Breast mass classification based on supervised contrastive learning and multi-view consistency penalty on mammography,” *IET Biometrics*, vol. 11, no. 6, pp. 588–600, 2022, doi: 10.1049/bme2.12076.
- [6] K. Akila, L. S. Jayashree, and A. Vasuki, “Mammographic image enhancement using indirect contrast enhancement techniques – A comparative study,” *Procedia - Procedia Comput. Sci.*, vol. 47, pp. 255–261, 2015, doi: 10.1016/j.procs.2015.03.205.
- [7] J. Y. Kim, L. S. Kim, and S. H. Hwang, “An advanced contrast enhancement using partially overlapped sub-block histogram equalization,” *IEEE Trans. Circuits Syst. Video Technol.*, vol. 11, no. 4, pp. 475–484, 2001, doi: 10.1109/76.915354.
- [8] E. D. Pisano *et al.*, “Contrast limited adaptive histogram equalization image processing to improve the detection of simulated spiculations in dense mammograms,” *J. Digit. Imaging*, vol. 11, no. 4, pp. 193–200, 1998, doi: 10.1007/BF03178082.
- [9] Y. T. Kim, “Contrast enhancement using brightness preserving bi-histogram equalization,” *IEEE Trans. Consum. Electron.*, vol. 43, no. 1, pp. 1–8, 1997, doi: 10.1109/30.580378.
- [10] Z. Yao, Z. Lai, and C. Wang, “Image Enhancement Based on Equal Area Dualistic Sub-image and Non-parametric Modified Histogram Equalization Method,” *Proc. - 2016 9th Int. Symp. Comput. Intell. Des. Isc. 2016*, vol. 1, no. 1, pp. 447–450, 2016, doi: 10.1109/ISCID.2016.1110.
- [11] S. Der Chen and A. R. Ramli, “Contrast enhancement using recursive mean-separate histogram equalization for scalable brightness preservation,” *IEEE Trans. Consum. Electron.*, vol. 49, no. 4, pp. 1301–1309, 2003, doi: 10.1109/TCE.2003.1261233.
- [12] S. Saravanan and R. Karthigaivel, “A fuzzy and spline based dynamic histogram equalization for contrast enhancement of brain images,” *Int. J. Imaging Syst. Technol.*, vol. 31, no. 2, pp. 802–827, 2021, doi: 10.1002/ima.22483.
- [13] M. Sundaram, K. Ramar, N. Arumugam, and G. Prabin, “Histogram based contrast enhancement for mammogram images,” *2011 - Int. Conf. Signal Process. Commun. Comput. Netw. Technol. ICSCCN-2011*, no. Icsccn, pp. 842–846, 2011, doi: 10.1109/ICSCCN.2011.6024667.
- [14] M. Sundaram, K. Ramar, N. Arumugam, and G. Prabin, “Histogram modified local contrast enhancement for mammogram images,” *Appl. Soft Comput. J.*, vol. 11, no. 8, pp. 5809–5816, 2011, doi: 10.1016/j.asoc.2011.05.003.
- [15] K. Panetta, Y. Zhou, S. Agaian, and H. Jia, “Nonlinear unsharp masking for mammogram enhancement,” *IEEE Trans. Inf. Technol. Biomed.*, vol. 15, no. 6, pp. 918–928, 2011, doi: 10.1109/TITB.2011.2164259.
- [16] S. C. Huang, F. C. Cheng, and Y. S. Chiu, “Efficient contrast enhancement using adaptive gamma correction with weighting distribution,” *IEEE Trans. Image Process.*, vol. 22, no. 3, pp. 1032–1041, 2013, doi: 10.1109/TIP.2012.2226047.
- [17] S. Rahman, M. M. Rahman, M. Abdullah-Al-Wadud, G. D. Al-Quaderi, and M. Shoyaib, “An adaptive gamma correction for image enhancement,” *Eurasip J. Image Video Process.*, vol. 2016, no. 1, pp. 1–13, 2016, doi: 10.1186/s13640-016-0138-1.
- [18] M. Kim and M. G. Chung, “Recursively separated and weighted histogram equalization for brightness preservation and contrast enhancement,” *IEEE Trans. Consum. Electron.*, vol. 54, no. 3, pp. 1389–1397, 2008, doi: 10.1109/TCE.2008.4637632.
- [19] S. Jenifer, S. Parasuraman, and A. Kadirvelu, “Contrast enhancement and brightness preserving of digital mammograms using fuzzy clipped contrast-limited adaptive histogram equalization algorithm,” *Appl. Soft Comput. J.*, vol. 42, pp. 167–177, 2016, doi: 10.1016/j.asoc.2016.01.039.
- [20] V. Magudeeswaran and K. Balasubramanian, “Fuzzy weighted histogram equalisation for contrast enhancement of mammogram images,” *Int. J. Biomed. Eng. Technol.*, vol. 28, no. 3, pp. 232–242, 2018, doi: 10.1504/IJBET.2018.095217.
- [21] C. Zhao, Z. Wang, H. Li, X. Wu, S. Qiao, and J. Sun, “A new approach for medical image enhancement based on luminance-level modulation and gradient modulation,” *Biomed. Signal Process. Control*, vol. 48, pp. 189–196, 2019, doi: 10.1016/j.bspc.2018.10.008.
- [22] H. Demirel, C. Ozcinar, and G. Anbarjafari, “Satellite image contrast enhancement using discrete wavelet transform and singular value decomposition,” *IEEE Geosci. Remote Sens. Lett.*, vol. 7, no. 2, pp. 333–337, 2009.
- [23] F. Kallel and A. Ben Hamida, “A New Adaptive Gamma Correction Based Algorithm Using DWT-SVD for Non-Contrast CT Image Enhancement,” *IEEE Trans. Nanobioscience*, vol. 16, no. 8, pp. 666–675, Dec. 2017, doi: 10.1109/TNB.2017.2771350.
- [24] A. K. Bhandari, A. Kumar, G. K. Singh, and V. Soni, “Dark satellite image enhancement using knee transfer function and gamma correction based on DWT–SVD,” *Multidimens. Syst. Signal Process.*, vol. 27, no. 2, pp. 453–476, 2016, doi: 10.1007/s11045-014-0310-7.
- [25] M. Zhou, K. Jin, S. Wang, J. Ye, and D. Qian, “Color Retinal Image Enhancement Based on Luminosity

- and Contrast Adjustment,” *IEEE Trans. Biomed. Eng.*, vol. 65, no. 3, pp. 521–527, 2018, doi: 10.1109/TBME.2017.2700627.
- [26] B. Gupta and M. Tiwari, “Color retinal image enhancement using luminosity and quantile based contrast enhancement,” *Multidimens. Syst. Signal Process.*, 2019, doi: 10.1007/s11045-019-00630-1.
- [27] G. Palanisamy, P. Ponnusamy, and V. P. Gopi, “An improved luminosity and contrast enhancement framework for feature preservation in color fundus images,” *Signal, Image Video Process.*, vol. 13, no. 4, pp. 719–726, 2019, doi: 10.1007/s11760-018-1401-y.
- [28] A. Gandhamal, S. Talbar, S. Gajre, A. F. M. Hani, and D. Kumar, “Local gray level S-curve transformation – A generalized contrast enhancement technique for medical images,” *Comput. Biol. Med.*, vol. 83, pp. 120–133, 2017, doi: 10.1016/j.compbiomed.2017.03.001.
- [29] H. El Malali, A. Assir, V. Bhateja, A. Mouhsen, and M. Harmouchi, “A Contrast Enhancement Model for X-Ray Mammograms Using Modified Local s-Curve Transformation Based on Multi-Objective Optimization,” *IEEE Sens. J.*, vol. 21, no. 10, pp. 11543–11554, 2021, doi: 10.1109/JSEN.2020.3028273.
- [30] M. Pawar and S. Talbar, “Local entropy maximization based image fusion for contrast enhancement of mammogram,” *J. King Saud Univ. - Comput. Inf. Sci.*, vol. 33, no. 2, pp. 150–160, 2021, doi: 10.1016/j.jksuci.2018.02.008.
- [31] A. A. Siddiqi, A. Khawaja, and A. Hashmi, “A novel fuzzy blend scheme for image enhancement of CT scans bearing liver cancer,” *Comput. Methods Biomech. Biomed. Eng. Imaging Vis.*, vol. 00, no. 00, pp. 1–6, 2021, doi: 10.1080/21681163.2021.1899853.
- [32] P. Kandhway, A. K. Bhandari, and A. Singh, “A novel reformed histogram equalization based medical image contrast enhancement using krill herd optimization,” *Biomed. Signal Process. Control*, vol. 56, p. 101677, 2020, doi: 10.1016/j.bspc.2019.101677.
- [33] D. P. Tripathi, K. Pragmaash, and U. R. Jena, “Differential Mean Deviation Factor based Contrast Enhancement Technique Using DWT-SVD for Non-Contrast CT Scan Images,” vol. 12, no. 10, pp. 1685–1692, 2021.
- [34] A. Khmag, A. R. Ramli, and N. Kamarudin, “Clustering-based natural image denoising using dictionary learning approach in wavelet domain,” *Soft Computing*, vol. 23, no. 17, pp. 8013–8027, 2019, doi: 10.1007/s00500-018-3438-9.
- [35] A. Khmag, “Digital image noise removal based on collaborative filtering approach and singular value decomposition,” *Multimed. Tools Appl.*, 2022, doi: 10.1007/s11042-022-12774-7.
- [36] P. S. J.-D. Mammo and undefined 1994, “The mammographic image analysis society digital mammogram database,” *ci.nii.ac.jp*, Accessed: Feb. 01, 2021. [Online]. Available: <https://ci.nii.ac.jp/naid/10005112488/>.
- [37] U. K. Acharya and S. Kumar, “Directed searching optimized texture based adaptive gamma correction (DSOTAGC) technique for medical image enhancement,” *Multimed. Tools Appl.*, vol. 83, no. 3, pp. 6943–6962, 2023, doi: 10.1007/s11042-023-15953-2.
- [38] S. Z. Ramadan, “Methods Used in Computer-Aided Diagnosis for Breast Cancer Detection Using Mammograms: A Review,” *J. Healthc. Eng.*, vol. 2020, 2020, doi: 10.1155/2020/9162464.